Macro and microscale Engineering Response of Rigid-Soft Gravel-Rubber Inclusions: Insights from Detailed Laboratory and DEM Numerical Investigations

Gabriele Chiaro (ORCID)**, Ali Tasalloti** (ORCID)**, Kevin Chew, Jayan S. Vinod** (ORCID)**, and Krishna Allulakshmi**

Abstract This paper summarizes the main results of a broader research activity aimed at facilitating the use of gravel-rubber mixtures (GRMs) in geotechnical engineering applications. Precisely, the results of direct shear tests carried out on three GRMs having different aspect ratios (AR = 0.28, 0.57, and 0.66) and prepared at different volumetric rubber contents (VRC = 0, 10, 25, 40, and 100%) are reported and discussed. Additionally, an original 3D hybrid DEM numerical model (named DEM4GRM model) for rigid-soft particle mixtures is presented, and its performance is evaluated. Lastly, using newly proposed micromechanical equations, factors such as fabric and force anisotropy, and strong-force chains are systematically examined throughout the shearing process to gain insight on the particle-level behavior of mixtures with varying VRC.

Keywords Gravel-rubber mixtures · Direct shear · DEM · Micromechanics

1 Introduction

In Australasia, geotechnical engineers are increasingly expected to meet requirements for environmentally friendly design, construction, and innovation [1]. As a result, reuse and recycling of construction and demolition materials, commercial wastes and industrial by-products in geotechnical engineering applications are progressively sought as it provides substantial benefits in terms of increased sustainability and reduced environmental impacts [2–6; among others]. Specifically, to the New Zealand context, due to the large number of waste tires produced annually

G. Chiaro (✉) · A. Tasalloti · K. Chew
Department of Civil and Natural Resources Engineering, University of Canterbury, Christchurch, New Zealand
e-mail: gabriele.chiaro@canterbury.ac.nz

J. S. Vinod · K. Allulakshmi
School Civil Mining Environmental Engineering, University of Wollongong, Wollongong, Australia

[7] and the need to design more seismic resilient structures [8], the recycling of tire-derived aggregates (TDAs) mixed with granular soils to produce lightweight fill materials with excellent mechanical and energy adsorption properties is of great significance [9].

A comprehensive literature review compiled by Tasalloti et al. [10] has shown that much of the previous research on granular mixtures has focused on the mechanical characterization of sand-rubber mixtures. Yet, in the selection of the soil type and recycled rubber size to form soil-rubber mixtures for use in geotechnical applications, the availability and the cost efficiency of both materials should be carefully considered [11]. In fact, to avoid inherent segregation of binary mixtures made of large and small particles [12, 13], the recycled rubber should be cut into smaller (sand size-like) pieces when mixed with sandy soils, which unavoidably increases the implementation costs. Consequently, as an alternative, the use of gravel-rubber mixtures (GRMs) has been increasingly recommended by researchers [14–20].

Nevertheless, compared to sand-rubber mixtures, the mechanical behavior of GRMs is still largely unknown. Therefore, as a part of a research activity aimed at facilitating, the use of GRMs is geotechnical applications in New Zealand [9, 15, 18, 20, 21], two subsequent steps were undertaken by the authors: (i) a number of direct shear investigations were carried out on three gravel-granulated rubber composites mixed at volumetric rubber content (*VRC*) of 0, 10, 25, 40 and 100% to evaluate the combined effects of *VRC*, aspect ratio ($AR = D_{50,R}/D_{50,G}$) and applied normal stress on the strength properties of GRMs; and (ii) a novel three-dimensional hybrid discrete element method model (named DEM4GRM) able to accurately describes the macromechanical direct shear response of rigid-soft particle mixtures was developed. Moreover, ad hoc equations defining key micromechanical features of such synthetic materials throughout the shearing processes were established for GRMs. In this paper, experimental findings are first summarized. Then, the new DEM4GRM model [22] is briefly introduced and simulation results are shown. Finally, using the newly proposed equations, microscale aspects such as fabric and force anisotropy and strong-force chains are scrutinized throughout the shearing process and compared among mixtures with varying *VRC*.

2 Experimental Study

2.1 Materials and Procedure

The strength properties of GRMs were estimated by means of a medium-size direct shear box (100×100 mm in cross-section and 53 mm in height) under three normal stress (σ_n) levels of 30, 60 and 100 kPa. The horizontal displacement rate was 1 mm/min.

Three types of rigid-soft granular mixtures were prepared by mixing a uniformly-graded rounded gravel (G) and three recycled rubber particle sizes: large (R1, $D_{50} =$
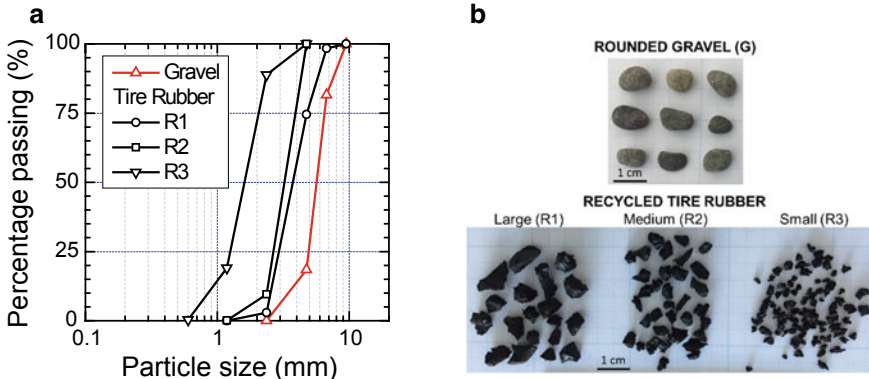
Fig. 1 **a** Particle size distribution curves and **b** photographic images of the gravel and granulated recycled tire rubber used in this study

3.74 mm), medium (R2, $D_{50} = 3.23$ mm), and small (R3, $D_{50} = 1.61$ mm). Figure 1 shows the particle size distribution curves and photographic images of each material. The material properties are listed in Table 1. The aspect ratio of the mixtures is G-R1 ($AR = 0.66$), G-R2 ($AR = 0.57$), and G-R3 ($AR = 0.28$). The GRMs were prepared at volumetric rubber contents (*VRC*) of 0, 10, 25, 40, and 100%, where *VRC* is defined as the ratio between the volume of rubber and the total volume of solids.

All specimens were tested in dry conditions and prepared at a degree of compaction of 90–95% (by dry tamping method), which was calculated based on the values of maximum dry density (ρ_{max}—obtained by standard proctor compaction tests). For completeness, the minimum dry density (ρ_{min}) was also determined by carefully pouring the materials in the compaction mold with zero depositional height. Note that vibratory table tests were found not effective to obtain ρ_{max} for GRMs. This is obviously in contrast to the response of typical hard-grained stiff granular materials for which vibratory compaction is most effective [23], but it can be attributed to the high energy absorption nature of the rubber particles in the mixtures.

Table 1 Properties of gravel and recycled tire rubber

Material	Gravel[**]	Recycled tire rubber		
		Large[**]	Medium[***]	Small[**]
Symbol	G	R1	R2	R3
Mean diameter, D_{50} (mm)	5.67	3.74	3.23	1.61
Specific gravity, G_s	2.71	1.15	1.15	1.14
Maximum dry density, ρ_{max} (kg/m³)*	1753	649	634	602
Minimum dry density, ρ_{min} (kg/m³)	1571	510	460	429

*by proctor compaction tests
[**]experimental data from Chiaro et al. [9, 21] and Tasalloti et al. [18, 20]
[***]experimental data from this study

Segregation is an inherent difficulty in granular mixtures that may be triggered by size, density, stiffness, and shape features [12]. Segregation in the GRM specimens was prevented by minimizing any vibration and avoiding granular flow.

2.2 Test Results

The materials investigated in this study are essentially binary granular mixtures consisting of rigid and soft particles of different size and shape. Their packing, density, and mechanical behavior are influenced by the inherent properties of the materials (i.e., size and shape), the proportion as well as the size ratio of large/small and rigid/soft particles in the total volume of solids.

2.2.1 Packing and Density Characteristics of GRMs

The variation of dry density (ρ_d) is shown in Fig. 2 for G-R1 and G-R3 mixtures. As the rubber particles are much lighter than the gravel grains (i.e., the G_s of gravel grains is more than twice than that of rubber particles), both the minimum and maximum dry densities of GRMs decrease almost linearly by increasing *VRC*. However, at *VRC* $\leq$ 40%, the dry density values of G-R3 are slightly above the linear trends. This is due to the fact that at lower *VRC*, small rubber particles can occupy the voids between large gravel grains (Fig. 2b) which results in an increase of the density state of the mixtures [12, 13]. In contrast, because the size of R1 particles is almost similar to that of the gravel, the rubber particles cannot fit in the voids between the gravel grains, even at lower *VRC*, but rather their replace the gravel grains in the mixtures (Fig. 2b).
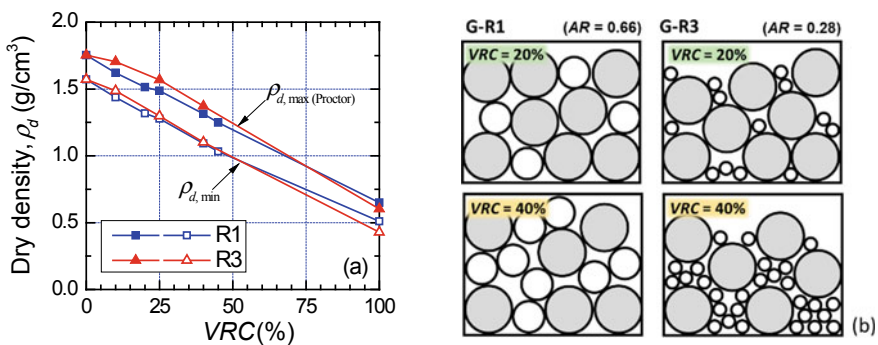

Fig. 2 Variation of **a** minimum and maximum dry density; and **b** idealized illustration of volume-biased packing of GRMs for *VRC* = 20 and 40%

2.2.2 Shear Strength Characteristics of GRMs

The stress–strain-volumetric behavior of G-R2 obtained by direct shear tests at σ_n = 30, 60, and 100 kPa is reported in Fig. 3. It can be seen that irrespective of σ_n, by increasing *VRC*, the material response gradually changes from dilative with a clear peak shear state to contractive without peak shear state. Moreover, the peak shear stress (τ_{max}) increases with increasing σ_n and decreases with decreasing *VRC*. Similar tendencies were observed for G-R1 and G-R3 (due to page limitation, not all the experimental data could be reported here but can be found in Tasalloti et al. [18, 20]). The summary plot reported in Fig. 4a shows that τ_{max} decreases with *AR*. Moreover, it indicates that the effects of *AR* on the GRM strength are less significant as compared to those due to *VRC* and σ_n.

Figure 4b reports the values of the Mohr–Coulomb friction angle (ϕ') for all mixtures. Essentially, ϕ' decreases significantly with increasing *VRC* (and only slightly with *AR*) from about 54° (gravel) to 29° (graduated rubber). Notably, excluding G-R2 and G-R3 with *VRC* > 85% and G-R1 with *VRC* > 95%, most of the GRMs have a high strength (i.e., ϕ'> 30°) irrespective of the *VRC* and rubber particle size making them suitable structural fill materials for many geotechnical applications [2, 9].
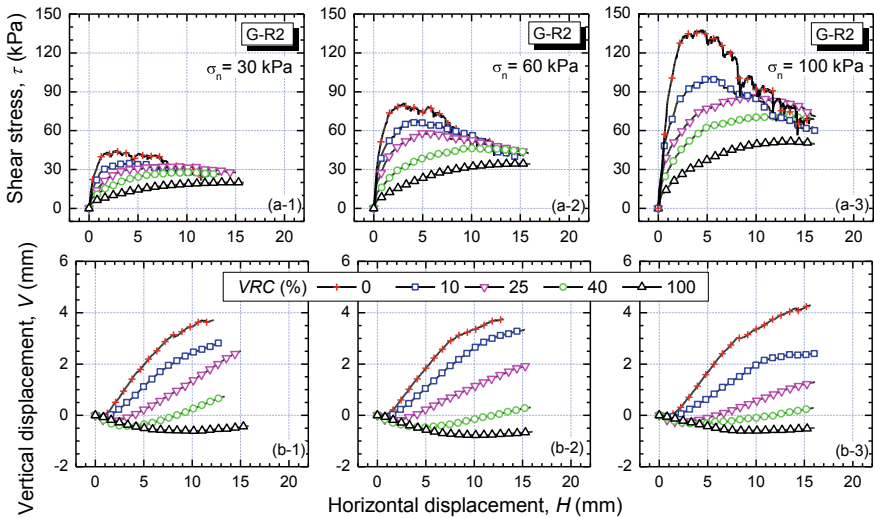

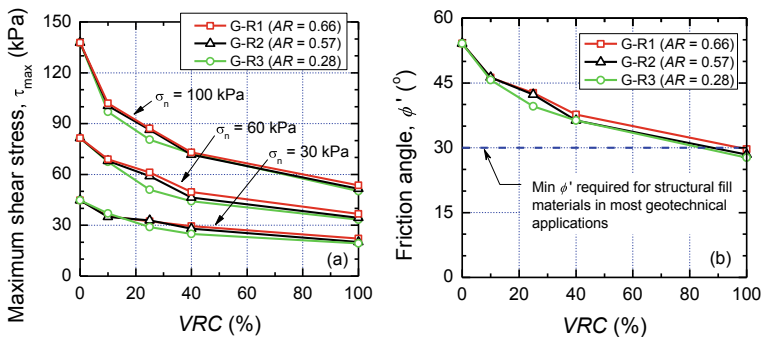**Fig. 3** G-R2 behavior in direct shear tests at 30, 60, and 100 kPa normal stress

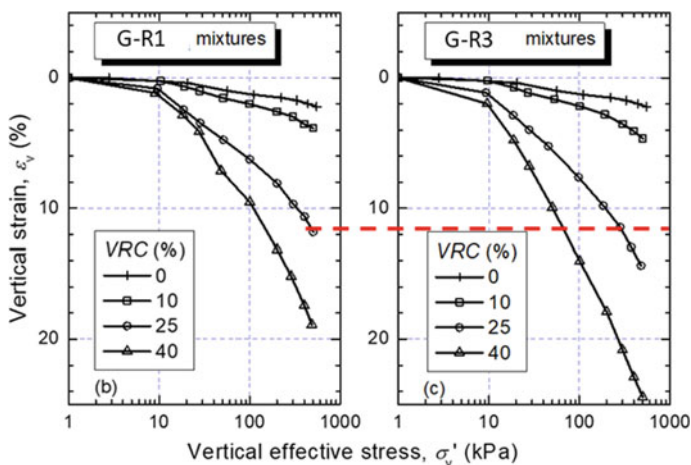**Fig. 4** **a** Maximum shear stress and **b** friction angle of GRMs in direct shear tests

Fig. 5 Compressibility of GRMs in one-dimensional compression tests with two-hour creep loading stages

2.3 Key Aspects to Consider in the Selection of GRMs

2.3.1 Compressibility

Despite the adequate strength of GRMs, the ultimate adoption of GRMs as structural fills in geotechnical application would depend also on their compressibility under sustained loads. Typical results obtained for G-R1 and G-R3 by one-dimensional compression tests with two-hour creep loading stages [21]. It is obvious that the higher is the vertical stress applied on GRMs, the higher is the vertical strain developed, and the lower is the *VRC* that may be accepted in the mixtures to satisfy compressibility requirements [18, 20]. Moreover, *AR* also plays a key role; in fact, for any combination of *VRC* and vertical stress, it can be seen that the mixtures

with small rubber particles (G-R3) experience large vertical strain as compared to those with large rubber particles (G-R1). Therefore, to have GRMs with enhanced compressibility, gravel and rubber particles with similar grain size should be used.

2.3.2 Environmental Implications

The introduction of new or alternative (recycled waste) materials in geotechnical applications may have benefits in terms of cost reductions and increased performance. However, it is essential to ensure that such innovations do not result in long-term negative impacts on the environment, e.g., through the leaching of toxic chemicals into the surrounding soil environment, groundwater, and surface water. The results of leaching tests conducted by Banasiak et al. [24] on GRMs have indicated that the leachate from smaller tire particles (R3) had a higher content of metals (e.g., Zn), as compared to the large rubber one (R1), implying that particle size and surface area influence the concentration of elements in tire-gravel mix leachate. To minimize the leaching of metals, therefore, the use of large rubber particle size is desirable.

3 DEM Numerical Modeling of GRMs

The discrete element method (DEM) is a very useful tool to investigate particle-level interactions and develop a better understanding of the macro and micromechanical behavior of granular matters [25]. Due to the granular and discrete nature of GRMs, DEM is indeed an ideal numerical modeling method to investigate the micromechanical behavior of such materials. Yet, the soft and low modulus nature of the rubber particles challenge one of the fundamental hypothesis of DEM by particle rigidity. Based on this hypothesis, contact forces are determined from the overlap between contacting bodies but the particles do not deform [25]. While the rubber softness may be accounted for by prescribing a low material stiffness, the volumetric behavior of pure rubber ($\nu^{\text{rubber}} = 0.5$) cannot be replicated easily in DEM using the particle rigidity method.

To address this issue, Asadi et al. [26] implemented a deformable agglomerate to model more accurate changes in the shape (deformation) of rubber particles by using weak internal bonds between tire rubber particles, allowing the spheres within a cluster to move and rearrange. In the following, Ren et al. [27] implemented a deformable single rubber particle model that is able to describe the volumetric behavior of rubber. It has been indicated that with sufficient rows of bonded spheres packed in a body-centered cubic (BCC) arrangement, this model can consistently and precisely capture the strength and volumetric response of a single rubber particle as the nonlinear mechanical behavior of rubber is described by a piecewise linear contact/bond model.

Taking advantage of both the well-established particle rigidity approach applicable to rigid gravel grains and the possibility to capture the soft rubber behavior using

BCC deformable particles, in this study, a 3D hybrid DEM model for GRMs (called DEM4GRM model) was developed using the particle flow code three-dimensional program (PFC3D, version 6.1 [28]). Such model makes it possible to explore the micromechanical direct shear behavior of GRMs under varying *VRC* and normal stress levels.

The framework in PFC3D is based on the DEM formulation by Cundall and Strack [29], where an explicit numerical scheme is used to monitor the interaction of particles individually and its corresponding contacts with neighboring particles. Moreover, based on the particle rigidity approach, contact forces are evaluated from the overlap between contacting bodies but the particles do not deform [25]. In this study, the Hertz-Mindlin contact law [30] was used to define the particle interaction at each contact. It is based on a nonlinear contact force-overlap relationship. The DEM4GRM model input parameters defining the contacts are provided in Table 2. As the gravel and rubber particles have different engineering properties, the surface property inheritance functionality in PFC3D [28] was used to determine hybrid contact properties between the gravel and rubber particles.

Table 2 DEM4GRM model: input parameters for G-R1 mixtures

Item	Parameter	Units	Value
Gravel	Particle density	kg/m^3	2710
	Coefficient of friction		0.72
	Shear modulus	MPa	90
	Poisson's ratio		0.3
Rubber	Particle density	kg/m^3	1150
	Coefficient of friction		0.27
Rubber–bonds	Shear modulus bonded spheres	MPa	12
	Bond elastic modulus	MPa	20
	Normal-to-shear stiffness ratio (k_n/k_s)		4.0
	Tensile strength	Pa	30E200
	Shear strength	Pa	30E200
	Critical damping ratio		0.25
Wall	Coefficient of friction		0.70
	Shear modulus	MPa	80,000
	Poisson's ratio		0.25
Global	Damping coefficient		0.2

3.1 Features of the DEM4GRM Model

3.1.1 Single Rubber Particles Model

Knowing the importance of accounting for the compressive volumetric behavior of rubber, an improved tire rubber particle model was proposed in this study, which builds on the studies from Asadi et al. [26] and Ren et al. [27]. Precisely, to attain an accurate simulation setup and reduced computation time, the BCC rubber model by Ren et al. [27] was enhanced and optimized. Figure 6a displays the proposed rubber model consisting of a cluster of 35 balls, BCC packed, and bonded together by linear parallel bonds [31]. The intercluster nonbond contacts, which would form when in contact with external particles, are defined using the Hertz-Mindlin model [30]. To guarantee that the compressive load is applied more evenly, an outer shell was positioned on each side of the cubic assembly. The model elastic parameters were defined using the results of a series of uniaxial compression tests on single
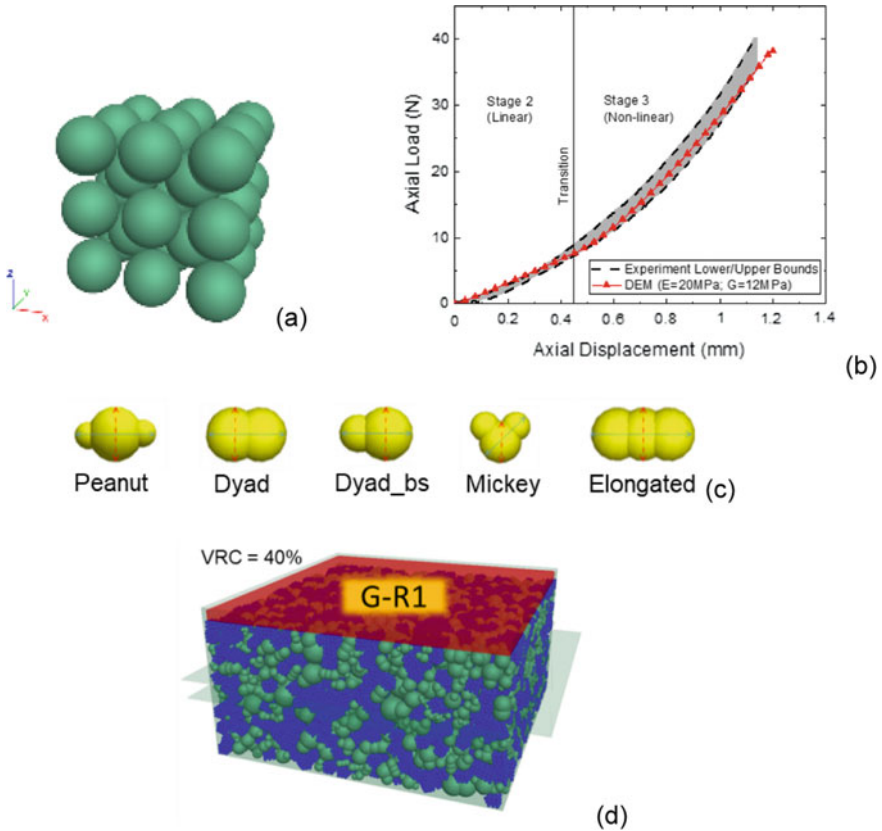

Fig. 6 Characteristics of the newly proposed DEM4GRM model

tire rubber particles as shown in Fig. 6b. Full details of the proposed single rubber particle model are available from Chew [32].

3.1.2 Gravel Particle Model

Due to the gravel particles size and shape variability, gravel grains were modeled using a simple clump shapes (Fig. 6c) as those considered by Garzia and Bray [33].

3.1.3 DEM Modeling of GRMs

The GRM specimens were generated using the overlapping method [28, 34] based on the particle size distribution of gravel and large rubber particles (R1) used in the laboratory experiments (Fig. 1). The specimens were quasi-statically compressed until reaching the required target degree of compaction. The normal stress was applied to the specimens by means of a force applied on the top plate. In the following, the specimens were sheared by moving the lower box at a rate of 0.002 m/s (to maintain quasi-static condition). Frictionless lateral walls were adopted to minimize k_0 effects. Figure 6d shows a typical DEM specimen obtained for $VRC = 40\%$.

The model parameters for the reference materials were determined by simulating the gravel ($VRC = 0\%$) and rubber ($VRC = 100\%$) behavior in direct shear tests and fitting the shear and volumetric response that best match the experimental direct shear results. No additional model parameters were defined for mixtures with $VRC = 10, 25$, and 40%, but rather the shear and volumetric trends in the simulations were merely defined by the proportion of gravel and rubber particles in the mixtures and the normal stress level applied on the specimens.

3.2 Simulation Results

In Fig. 7a, b, typical DEM simulation results are presented for gravel and granulated rubber specimens, respectively, sheared at $\sigma_n = 30, 60$, and 100 kPa. It can be seen that irrespective of the stress level, there is a very good agreement with the experimental tests results, both in terms of stress and volumetric behaviors.

Moreover, the results obtained for GRMs sheared at $\sigma_n = 100$ kPa are reported in Fig. 7c. Despite no explicit model parameters were defined for the mixtures, there is a good agreement with the experimental tests results, being the model capable of capturing key futures of dilative (rigid gravel-like) and compressive (soft rubber-like) mixture responses with varying VRC. Yet, while the stress response is perfectly described, the volumetric response appears to be slightly overpredicted, although the trends are correct (i.e., showing a more contractive behavior with increasing VRC).
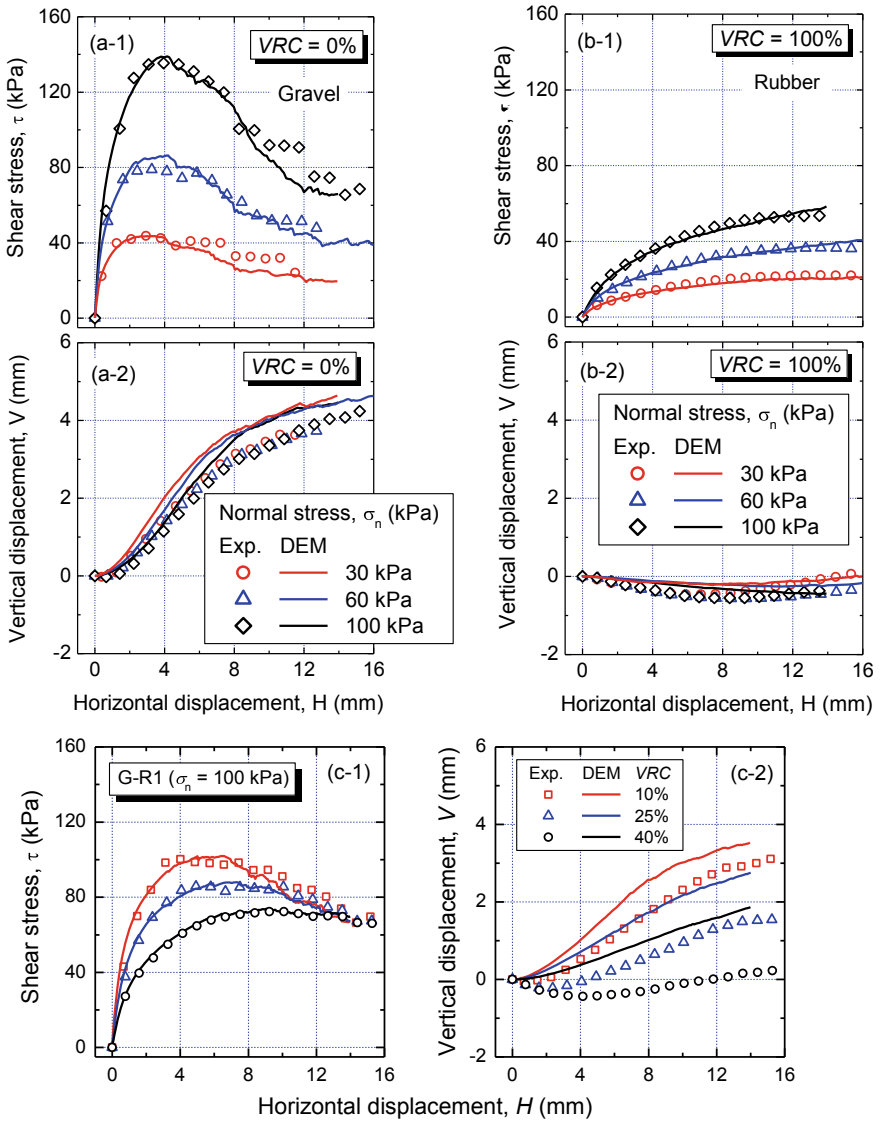
Fig. 7 DEM4GRM simulation results for: **a** gravel specimens; **b** granulated rubber specimens; and **c** G-R1 specimens

4 Micromechanics Analyzes and Discussion

4.1 Fabric and Force Anisotropy

The methodology proposed by Rothenburg and Bathurst [35] was used to quantify the fabric and force anisotropy in the DEM4GRM model simulations during shearing with some modifications in line with the latest research outcomes (e.g., [36]). A curve fitting approach using second-order Fourier series yielded the following expressions that best describe the (polar) distribution of different contact types considered in this study. The shape of the distribution of the contact vector—fabric can be approximated using the harmonic function:

$$E(\theta) = \frac{\{1 + a \cos 2(\theta - \theta_a)\}}{2\pi} \tag{2.1}$$

where a represents the magnitude or coefficient of anisotropy of the contact orientations, and θ_a is the principal direction of this anisotropy. Similarly, the contact normal force distribution can be represented by

$$\overline{f}_n(\theta) = \overline{f}_n^o \{1 + a_n \cos 2(\theta - \theta_n)\} \tag{2.2}$$

where $\overline{f}_n^o$ is the average contact normal force, a_n is the parameter describing the anisotropy of the contact normal force component, and θ_n is the direction of the maximum average normal forces. The expressions in Eqs. (2.1) and (2.2) are found to be similar to those used by Rothenburg and Bathurst [35].

The following expression was proposed to best approximate the tangential force distribution for the GRMs considered in this study:

$$\overline{f}_t(\theta) = \overline{f}_t^o \{1 + a_t \cos 4(\theta - \theta_t)\} \tag{2.3}$$

where $\overline{f}_t^o$ is the average contact shear force, a_t is the parameter describing the anisotropy of the contact tangential force component, and θ_t defines the direction of the peak contact shear force. Note that this expression differs to that reported by Rothenburg and Bathurst [35], by which the tangential force approaches zero between the peaks. This is due to the fact that Rothenburg and Bathurst [35] considered perfect spheres whereas in this study clumps were used. The interlocking effects introduced by the clumps give rise to "background" tangential forces that are randomly orientated, and thus, the tangential forces do not diminish along orthogonal planes. The resultant tangential force distribution is akin to a superposition of an isotropic "background" tangential forces (Eq. 3), which forms a slightly different distribution to that observed by Rothenburg and Bathurst [35].

Figure 8 shows the comparison between polar histograms of the fabric, normal force and tangential force distribution at different shearing stages obtained by the proposed approximation functions, and DEM simulations for GRMs ($VRC = 25\%$ at $\sigma_n = 60$ kPa). For inclusiveness, the variation during the shearing process of the force anisotropy coefficients (a, a_n, and a_t) is also reported. Although not presented here, it is important to mention that very similar trends were obtained at 30 and 100 kPa normal stress.

Generally, the fabric of the rubber ($VRC = 100\%$) specimens is significantly different from that of the gravel ($VRC = 0\%$) and that of the mixtures look like one or the other depending on the VRC content. Specifically, at $VRC = 40\%$, the trends in a, a_n, and a_t begin to be similar to that of $VRC = 100\%$, suggesting that the soft-like rubber-dominated behavior is expected for the mixtures with $VRC \geq 40\%$. Contrarily, the peaks in a, a_n, and a_t coefficients trends during shearing are obvious up to $VRC = 25\%$, suggesting that rigid-like gravel-dominated behavior is expected for the mixtures with $VRC \leq 25\%$. This was confirmed by the analysis of the force network as described in the next section.
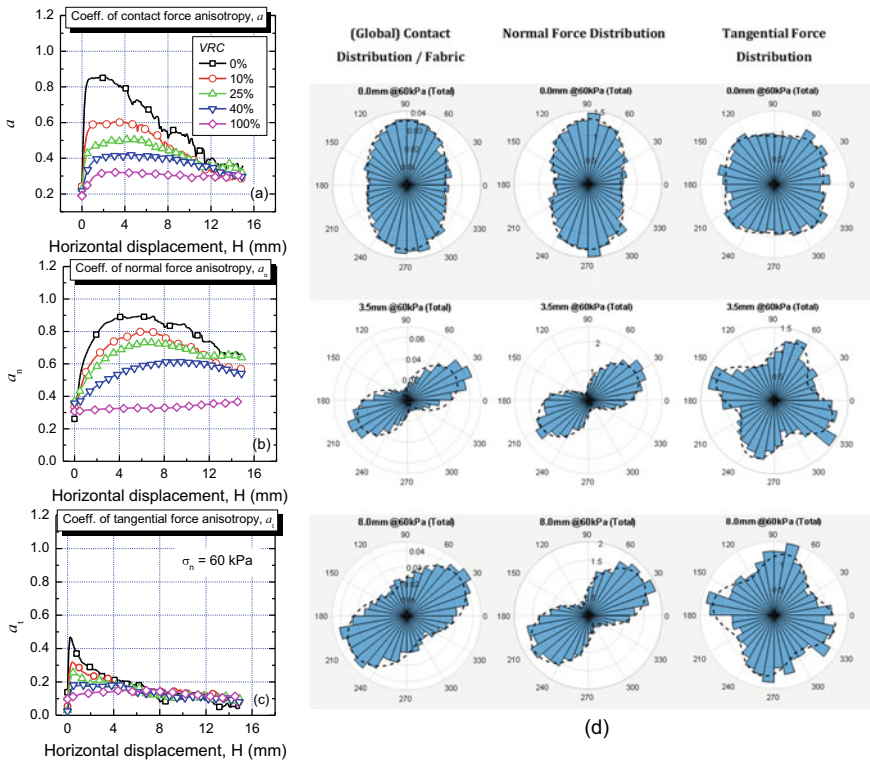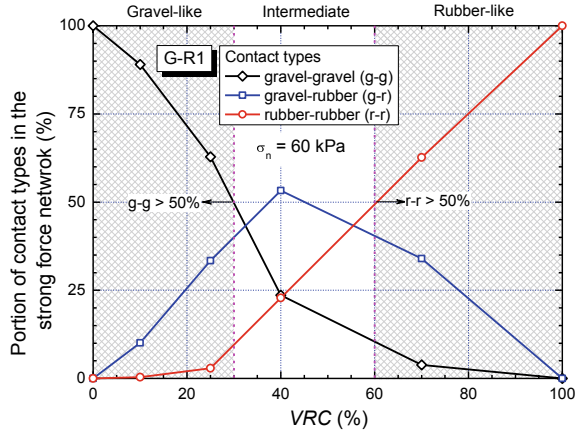

Fig. 8 Variation of force anisotropy coefficients with VRC at 60 kPa normal stress: **a** contact force; **b** normal force; **c** tangential force; and **d** polar histograms ($VRC =25\%$)

Fig. 9 Behavioral zones for GRMs in direct shear tests

4.2 Force Network

It has been well established that the contact network can be separated into two categories: the strong force network and the weak force network [37]. The strong force network consists of contact forces greater than the average force in the assembly and represents the load-bearing force chains that form during shearing and is responsible for the fabric and force anisotropy observed [36, 38, 39].

Figure 9 reports a typical distribution of the amount of gravel-gravel (g-g), gravel-rubber (g-r), and rubber-rubber (r-r) contacts participating in the strong force network for various GRMs. It can be observed that the proportion of r-r contacts in the strong force network is irrelevant up to $VRC = 25–30\%$, and more than half of the strong contacts are g-g contacts. From $VRC = 25\%$ onward, the proportion of strong r-r contacts increases significantly while the proportion of strong g-g force chains decrease rapidly. At $VRC = 40\%$, both the r-r and g-g contacts carry an equal proportion of the strong contacts. Yet, the strong forces chains are primarily transmitted via the g-r contacts, giving rise to an intermediate behavior where the specimen displays primarily a dilative behavior during shearing. The peak shear stress is also less pronounced. Above $VRC = 60\%$, r-r contacts sustain most of the strong-force chains in the assembly.

5 Concluding Remarks

In this paper, the results of direct shear tests carried out on gravel-rubber mixtures (GRMs)—having different aspect ratios (AR = 0.28, 0.57, and 0.66), prepared at different volumetric rubber contents ($VRC = 0, 10, 25, 40,$ and 100%) and sheared at 30, 60, and 100 kPa normal stress—were reported and discussed. Moreover, an original 3D hybrid DEM numerical model for rigid-soft particle mixtures was presented,

and its performance was assessed. Finally, using newly proposed constitutive equations, microscale factors such as fabric, force anisotropy, and strong force chains were systematically examined throughout the shearing process to gain insight on the micromechanical behavior of mixtures with varying *VRC*.

The following main conclusions can be drawn from this study:

Macroscale

(i)   Irrespective of the applied normal stress level and rubber particle size (or aspect ratio, *AR*), the response of GRMs changed rapidly from dilative-like to contractive-like with the addition of rubber in the mixtures;

(ii)   Independently from *AR*, the friction angle (ϕ') was found to be between 54° (gravel) and 29° (rubber) indicating that the majority of GRMs are suitable structural fill materials for most geotechnical applications ($\phi' \geq 30°$);

(iii)   The ultimate adoption of GRMs in geotechnical application depends also on their compressibility that may limit the *VRC* in the mixtures, especially when small rubber particles (or aspect ratios) are used to form GRMs%;

(iv)   From an environmental viewpoint, the use of GRMs with large rubber particle (free from steel wires) is desirable since it would minimize the leaching of toxic metals (e.g., Zn) from granulated rubber.

Microscale

(v)   Micro fabric and force anisotropy generally decreased with increasing *VRC*, following a similar pathway observed for the macroscale strength behavior;

(vi)   Based on the strong force network analysis, three distinct behavioral zones were identified for GRMs:

- gravel-like rigid behavior zone: VRC $\leq$ 30%;
- intermediate behavior/transition zone: 30% < VRC < 60%; and
- rubber-like soft behavior zone: VRC $\geq$ 60%.

It is important to mention that the above is valid for the level of normal stress considered in this study. In fact, at higher stress levels, the rubber-like behavior could become more predominant even at lower *VRC* levels.

References

1. Arulrajah, A., Narsilio, G., Kodikara, J., & Orense, R. P. (2015). Key issues in environmental geotechnics: Australia-New Zealand. *Environmental Geotechnics, 6*, 326–330.

2. Chiaro, G., Indraratna, B., Tasalloti, S. M. A., & Rujikiatkamjorn, C. (2015). Optimisation of coal wash–slag blend as a structural fill. *Ground Improvement, 168*(1), 33–44.

3. Tasalloti, S. M. A., Indraratna, B., Rujikiatkamjorn, C., Heitor, A., & Chiaro, G. (2015). A laboratory study on the shear behavior of mixtures of coal wash and steel furnace slag as potential structural fill. *Geotechnical Testing Journal, 38*(4), 361–372.

4. Mashiri, M. S., Vinod, J. S., Sheich, M. N., & Tsang, H. H. (2015). Shear strength and dilatancy behaviour of sand–tyre chip mixtures. *Soils and Foundations, 55*(3), 517–528.

5. Qi, Y., Indraratna, B., & Twak, M. (2020). Use of recycled rubber elements in track stabilisation. *Geotechnical Special Publication, GSP 319*, 49–59.

6. Ghorbani, B., Arulrajah, A., Narsilio, G., Horpibulsuk, S., & Bo, M. W. (2021). Dynamic characterization of recycled glass-recycled concrete blends using experimental analysis and artificial neural network modeling. *Soil Dynamic Earthquake Engineering 142*, 106544.

7. Ministry for the Environment. (2015). Waste tyres economic research. *Report 3*, pp. 87.

8. Hernandez, E., Palermo, A., Granello, G., Chiaro, G., & Banasiak, L. (2020). Eco-rubber seismic isolation foundation systems, a sustainable solution for New Zealand context. *Structural Engineering International, 30*(2), 192–200.

9. Chiaro, G., Tasalloti, A., Banasiak, L., Palermo, A., Granello, G., & Rees, S. (2020). Sustainable recycling of end-of-life tyres in civil (geotechnical) engineering applications: Turning issues into opportunities in the New Zealand context. *New Zealand Geomechanical News, 99*, 38–47.

10. Tasalloti, A., Chiaro, G., Murali, A., & Banasiak, L. (2021). Physical and mechanical properties of granulated rubber mixed with granular soils—a literature review. *Sustainability, 13*(8), 1–28, 4309.

11. Hazarika, H., & Abdullah, A. (2016). Improvement effects of two and three dimensional geosynthetics used in liquefaction countermeasures. *Japan Geotechnical Society Special Publication, 2*(68), 2336–2341.

12. Kim, H. K., & Santamarina, J. C. (2008). Sand-rubber mixtures (large rubber chips). *Canadian Geotechnical Journal, 45*, 1457–1466.

13. Lee, J. S., Doods, J., & Santamarina, J. C. (2007). Behavior of rigid-soft particle mixtures. *Journal of Materials in Civil Engineering, 19*(2), 179–184.

14. Pasha, S. M. K., Hazarika, K., & Yoshimoto, N. (2019). Physical and mechanical properties of gravel-tire chips mixture (GTCM). *Geosynthetics International, 26*(1), 92–110.

15. Chiaro, G., Palermo, A., Banasiak, L. J., & Granello, G. (2019). Direct shear behaviour of gravel-granulated tyre rubber mixtures. In: Proceedings of 13th ANZ Geomechanical Conference, Perth, Australia, 221–226.

16. Hazarika, H., Pasha, S. M. K., Ishibashi, I., Yoshimoto, N., Kinoshita, T., Endo, S., Karmokar, A. K., & Hitosugi, T. (2020). Tire-chip reinforced foundation as liquefaction countermeasure for residential buildings. *Soils and Foundations, 60*(2), 315–326.

17. Balaji, P. Dashti, S., & Liel, A. B. (2020). In-ground gravel–rubber panel walls to mitigate and base isolate shallow-founded structures on liquefiable ground. *Journal Geotechnical Geoenvironmental Engineering, 146*(9). https://doi.org/10.1061/(ASCE)GT.1943-5606.0002310

18. Tasalloti, A., Chiaro, G., Banasaik, L., & Palermo, A. (2021). Experimental investigation of the mechanical behaviour of gravel-granulated tyre rubber mixtures. *Construction and Building Matererials, 273*, 127149. https://doi.org/10.1016/j.conbuildmat.2020.121749

19. Pitilakis, D., Anastasiadis, A., Vratsikidis, A., Kapouniaris, A., Massimino, M. R., Abate, G., & Corsico, S. (2021). Large-scale field testing of geotechnical seismic isolation of structures using gravel-rubber mixtures. Earthquake Engineering and Structural Dynamics. https://doi.org/10.5281/zenodo.4557538

20. Tasalloti, A., Chiaro, G., Palermo, A., & Banasiak, L. J. (2020). Effect of rubber crumbs volumetric content on the shear strength of gravelly soil in direct shear apparatus. *Geotechnical Special Publications GSP, 319*, 259–266.

21. Chiaro, G., Palermo, A., Granello, G., Tasalloti, A., & Banasiak, L. J. (2021). Reuse of waste tires to develop eco-rubber seismic-isolation foundation systems: Preliminary results. *Lecture Notes in Civil Engineering, 144*, 159–169.

22. Chew, K., Chiaro, G., Tasalloti, A., Vinod, J., & Allulakshmi, K. (2021). Response of gravel-rubber mixtures under direct shear testing: experimental and DEM numerical investigation. In: Proceedings of 21st NZ Geotechnical Social Symposium, Dunedin, New Zealand, p. 10.
23. Iolli, S., Modoni, G., Chiaro, G., & Salvatore, E. (2015). Predictive correlations for the compaction of clean sands. *Transportation Geotechnics, 4*, 38–49.
24. Banasiak, L. J., Chiaro, G., Palermo, A., & Granello, G. (2021). Environmental implications of the recycling of end-of-life tires in seismic-isolation foundation systems. *Lecture Notes in Civil Engineering, 144*, 43–52.
25. O'Sullivan, C. (2011). *Particulate discrete element modelling: A geomechanics perspective.* Taylor & Francis.
26. Asadi, M., Mahboubi, A., & Thoeni, K. (2018). Discrete modeling of sand–tire mixture considering grain-scale deformability. *Granular Matter, 20*, 1–13.
27. Ren, Z. L., Cheng, Y. P., & Xu, X. (2020). A DEM method for simulating rubber tyres. *Géotechnique Letters, 10*, 73–79.
28. Itasca Consulting Group: Particle flow code in three dimensions—PFC3D (2018).
29. Cundall, P. A., & Strack, O. D. L. (1979). Discrete numerical model for granular assemblies. *Géotechnique, 29*(1), 47–65.
30. Mindlin, R. D., & Deresiewicz, H. (1953). Elastic spheres in contact under varying oblique forces. *Journal of Applied Mechanics, 20*, 327–344.
31. Potyondy, D. O., & Cundall, P. A. (2004). A bonded-particle model for rock. *International Journal of Rock Mechanics and Mining Sciences, 41*, 1329–1364.
32. Chew, K. (2021). *The mechanical behaviour of gravel-rubber mixtures: insights from DEM numerical investigations.* MEng Thesis, University of Canterbury, pp. 112.
33. Garcia, F. E., & Bray, J. D. (2019). Modeling the shear response of granular materials with discrete element assemblages of sphere-clusters. *Computers and Geotechnics, 106*, 99–107.
34. Zhang, M., Yang, Y., Zhang, H., & Yu, H. S. (2019). DEM and experimental study of bi-directional simple shear. *Granular Matter, 21*, 1–13.
35. Rothenburg, L., & Bathurst, R. J. (1989). Analytical study of induced anisotropy in idealized granular materials. *Géotechnique, 39*, 601–614.
36. Guo, N., & Zhao, J. (2013). The signature of shear-induced anisotropy in granular media. *Computers and Geotechnics, 47*, 1–15.
37. Radjai, F., Wolf, D. E., Jean, M., & Moreau, J. J. (1998). Bimodal character of stress transmission in granular packings. *Physical Review Letters, 80*, 61–64.
38. Huang, X., Hanley, K. J., O'Sullivan, C., & Kwok, C. Y. (2014). Exploring the influence of interparticle friction on critical state behaviour using DEM. *International Journal for Numerical and Analytical Methods in Geomechanics, 38*, 1276–1297.
39. Lopera Perez, J. C., Kwok, C. Y., & Senetakis, K. (2017). Investigation of the micro-mechanics of sand–rubber mixtures at very small strains. *Geosynthetics International, 24*, 30–44.